SCIENCE CHINA
Chemistry

• ARTICLES •

June 2017 Vol.60 No.6: 799–805
doi: 10.1007/s11426-016-0409-4

Mesoporous silica nanoparticles-assisted ruthenium(II) complexes for live cell staining

Jia Wen, Hui Yan, Pengyi Xia, Yongqian Xu, Hongjuan Li & Shiguo Sun*

Shaanxi Key Laboratory of Natural Products & Chemical Biology, School of Chemistry & Pharmacy, Northwest Agriculture and Forestry University, Yangling 712100, China

Received October 5, 2016; accepted December 13, 2016; published online February 27, 2017

Ruthenium complexes which can bind to DNA via electrostatic and intercalation interactions producing strong luminescence have become ideal candidates for DNA staining. However, some of them such as $Ru(phen)_3Cl_2$ and $Ru(phen)_2(dppz)Cl_2$ could hardly cross the cellular membrane of live cells which limited their further interaction with DNA in live cells. To solve this problem, a potential approach is to find a proper vehicle for loading and delivery of these ruthenium complexes into live cells. Mesoporous silica nanoparticles (MSNs) with non-toxicity and good biocompatibility can be good candidates. More importantly, ruthenium complexes with positively charge could be loaded on negatively charged MSNs via electrostatic attractions to form MSNs-Ru hybrid. *In vitro* test demonstrated that MSNs had no side effects on the interactions between Ru complexes and DNA. Furthermore, it is found that the MSNs-Ru hybrid can enter into living human cervical cancer cells HeLa and stain the DNA while the corresponding ruthenium complexes alone could hardly cross the cellular membrane in the control experiment, demonstrating MSNs can be employed to be an efficient ruthenium complexes delivery nanomaterial for live cell staining.

ruthenium complexes, mesoporous silica, DNA imaging

Citation: Wen J, Yan H, Xia P, Xu Y, Li H, Sun S. Mesoporous silica nanoparticles-assisted ruthenium(II) complexes for live cell staining. *Sci China Chem*, 2017, 60: 799–805, doi: 10.1007/s11426-016-0409-4

1 Introduction

As the library that cells use to store and execute the information required for life, DNA is the key molecule for the operation of almost all biological systems [1]. In order to study the physiological activities associated with DNA better, visualization is indispensable. As a consequence, enormous methods have been developed for DNA imaging or staining. Among them, fluorescent/luminescent probes are commonly used in molecular biology and analytical chemistry [2–6]. And the vast majority of the available cell staining dyes are based on organic molecules [7–10] and transition metal complexes [11–17]. For example, ruthenium complexes such as $Ru(phen)_3Cl_2$, $Ru(phen)_2(dppz)Cl_2$ (where phen=1,10-phenanthroline, and dppz=dipyridophenazine, Figure 1) which can bind to DNA via electrostatic and intercalation interactions producing strong luminescence have become ideal candidates for DNA staining [18–23].

However, it should be noted that $Ru(phen)_3Cl_2$, $Ru(phen)_2(dppz)Cl_2$, etc. can only cross the membrane of fixed cells or dead cells but bears poor uptake by live cells, which definitely limits their further application to some extent [21,23–28]. To solve this problem, a potential approach is to find a proper vehicle to load and delivery these ruthenium complexes into living cells. In our previous work, graphene oxide (GO) has been exploited as an efficient nanovector for loading and delivery of $Ru(phen)_3Cl_2$ into living cells and it is found that the GO-Ru hybrid can enter into the nuclei and stain the DNA of living human breast can-

*Corresponding author (email: sunsg@nwsuaf.edu.cn)

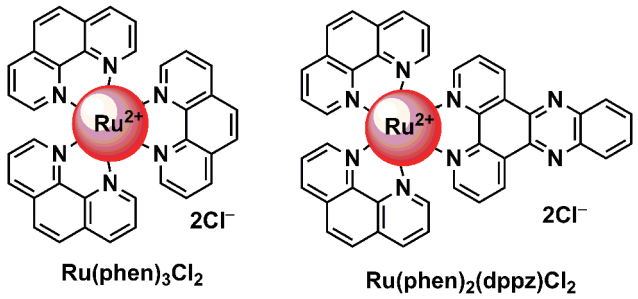

Figure 1 The structure of $Ru(phen)_3Cl_2$ and $Ru(phen)_2(dppz)Cl_2$ (color online).

cer cells MCF-7, while $Ru(phen)_3Cl_2$ alone cannot cross the cellular membrane in the control experiment [29]; GO also has been exploited as an efficient nano-vehicle for loading and delivery of propidium iodide (PI) into live cells to stain DNA (or RNA) [30]. Furthermore, an organic compound, Cucurbit[7]uril (CB7), has been used to transport a near-infrared fluorescent dye Hsd to enter into live cells for selective RNA staining [31].

Mesoporous silica nanoparticles (MSNs) have drawn worldwide attention in the past decades owing to their unique properties, such as periodically aligned pore structure, easily modified inner/outer surfaces, high surface area and good biocompatibility [32–37]. And thus they have extensive potential applications in various important research fields, including separation, drug storage, adsorption, delivery, catalysis, energy conversion and nanofabrication, etc. [38–41]. Especially, MSNs have been widely used as nanocarriers for anti-cancer drug delivery systems [42–44]. All these provide evidence that MSNs can be employed as a vehicle for loading and delivery ruthenium complexes into living cells.

Herein, to continue our research on loading and delivery dyes which cannot cross live cells' membrane into live cells via appropriate vectors, MSNs were first synthesized according to the literature [45], then two typical positively charged ruthenium complexes, $Ru(phen)_3Cl_2$ and $Ru(phen)_2(dppz)Cl_2$ were selected as examples and used respectively to interact with surface negatively charged MSNs to form two physical adsorption MSNs-Ru hybrid materials (MSNs-$Ru(phen)_3Cl_2$ (MR-**1**) and MSNs-$Ru(phen)_2(dppz)Cl_2$ (MR-**2**)). It is noted that significant luminescence enhancements can be observed after addition of a certain amount of DNA into the corresponding solutions of MR-**1** and MR-**2**, which was similar with the interactions between ruthenium complexes alone and DNA, demonstrating that MSNs had no side effects on the interactions between ruthenium complexes and DNA, and just acted as vectors. More importantly, both of the MR-**1** and MR-**2** can cross the cell membrane and stain the DNA of living human cervical cancer cells HeLa efficiently (Scheme 1).

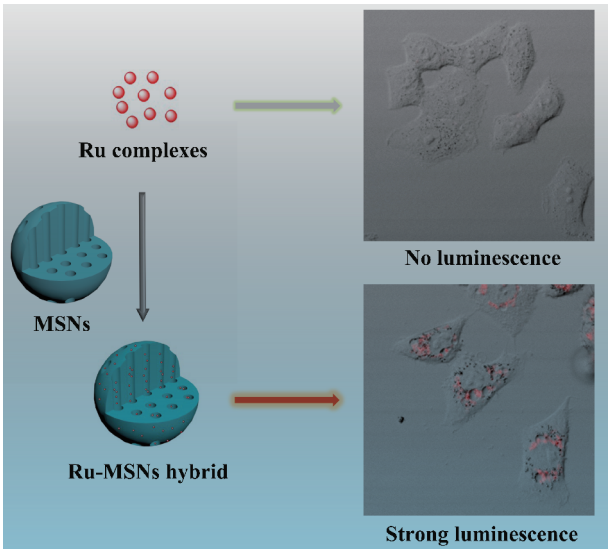

Scheme 1 Schematic demonstration of MSNs-Ru hybrid for live cell imaging (color online).

2 Experimental

2.1 Reagents and apparatus

All reagents were purchased from commercial suppliers and used without further purification unless specified. Anhydrous ethanol, ammonium hydroxide (25 wt% NH_3 in water), tetraethoxysilane (TEOS, 98%), cetyltrimethylammonium bromide (CTAB, 99%) and 5-diphenyltetrazolium bromide (MTT) were purchased from Aladdin Industrial Corporation (USA). Calf thymus DNA (ct-DNA) was purchased from Sigma Chemical Co. (USA). Ultrapure Milli-Q water (ρ>18.0 MΩ cm^{-1}) was used throughout the luminescence experiments. $Ru(phen)_3Cl_2$ and $Ru(phen)_2(dppz)Cl_2$ used in experiments were synthesized according to the literature procedure [46,47]. HeLa cells were maintained in Dulbecco's Modified Eagle's Medium (DMEM, Invitrogen, USA) with 10% (*v*/*v*) fetal bovine serum (FBS), 1% (*v*/*v*) penicillin/streptomycin.

Scanning electron microscope (SEM) images and the electron diffraction X-ray spectroscopy (EDS) were recorded with a Quanta 200 scanning electron microscope (Hitachi, Japan) operating at 200 kV. High-resolution transmission electron microscope (HRTEM) images, transmission electron microscope (TEM) mapping were recorded with a JEM-3010 transmission electron microscope (JEOL, Japan) operating at 200 kV. TEM images were obtained on a HT7700 instrument (Hitachi Ltd., Japan) at 80 kV. And specimens which were prepared through dispersing the samples into alcohol via ultrasonic treatment dropped on carbon-copper grids for observation. The emission spectra were collected using a 1750 UV-visible spectrometer (UV-Vis; Shimadzu, Japan) and a RF-5301 fluorescence spectrometer (Shimadzu, Japan),

respectively. Cell culture was carried out in an incubator with a humidified atmosphere of 5% CO_2 at 37 °C. Cell toxicity tests were tested by microplate reader (KHB ST-360, China). The confocal laser microscope data were acquired using a confocal fluorescence microscope (Nikon A1R, Japan).

All of the experiments were performed in compliance with the relevant laws and institutional guidelines, and were approved by Northwest Agriculture and Forestry University.

2.2 Preparation of MSNs

The MSNs particles were synthesized according to previous procedures with modification [45]. The synthesis of mesoporous silica spheres was achieved by the ammonia-catalyzed hydrolysis and condensation of TEOS in mixed ethanol-water solvents by using CTAB as surfactant. Typically, 0.08 g of the CTAB were dissolved in 40.5 mL mixture of water and ethanol solution (13 mL ethanol/27.5 mL water) and sonicated for 5 min, which was followed by the addition of 0.5 mL of ammonia solution under a stirring speed of 700 r/min at 25 °C for 30 min. The final concentration of CTAB was 5 mM. Then 0.5 mL of TEOS was dropwise added in the mixed solution and then stirred for another 3 h. The milk-white as-synthesized materials were collected by centrifugation, washed with water and ethanol several times respectively, and then vacuum drying. The products were calcined in air at 550 °C for 5 h to remove the template CTAB.

2.3 Preparation of the MR-1 and MR-2 hybrid

Stock solutions of $Ru(phen)_3Cl_2$ (1.0×10^{-2} M) and MSNs (1 mg/mL) were prepared separately in ultrapure water. 99 μL of the $Ru(phen)_3Cl_2$ solution was added to 3 mL of the MSNs solution. The mixed solution was stirred for 48 h at room temperature in the dark, then washed with ultrapure water for 3 times to remove the floating dye and then collected by centrifugation, and vacuum drying. To evaluate $Ru(phen)_3Cl_2$-loading capacity, the initial $Ru(phen)_3Cl_2$ solution and the supernatant and the washing solution after loading were collected. $Ru(phen)_3Cl_2$ content in the supernatant solution before or after incubation and washing solution after loading was measured by a UV-Vis spectrophotomete at λ=446 nm. The loading efficiency of $Ru(phen)_3Cl_2$ was estimated to be approximately 40.4%.

The preparation of MR-**2** was the same as MR-**1**. $Ru(phen)_2(dppz)Cl_2$ content in the supernatant solution before or after incubation and washing solution after loading was measured by a UV-Vis spectrophotomete at λ=440 nm. And the loading efficiency of $Ru(phen)_2(dppz)Cl_2$ was calculated to be 34.3%.

2.4 Luminescence experiments

Tri-HCl buffer (pH 7.4, 10.0 mM, Tris=tris(hydroxymethyl aminomethane)) was prepared using ultrapure water. Stock solution of ct-DNA (1.259×10^{-3} g/mL) was prepared by dissolving commercial ct-DNA in Tris-HCl buffer. Stock solutions of $Ru(phen)_3Cl_2$, $Ru(phen)_2(dppz)Cl_2$, MR-**1** and MR-**2** hybrid were prepared separately in ultrapure water. An aliquot of the $Ru(phen)_3Cl_2$, $Ru(phen)_2(dppz)Cl_2$, MR-**1** and MR-**2** hybrid stock solution was added to 3 mL of Tris-HCl buffer in a quartz cuvette separately. Then ct-DNA was added into the as-prepared solution until the highest luminescence intensity was reached. The sample was gently stirred for 5 s each time before the luminescence spectra were recorded. In all the titration experiments, the total volume was maintained not to exceed 5% of the original volume.

2.5 Confocal fluorescence microscopy

HeLa cells were seeded in 35 mm plastic bottomed μ-dishes for 24 h. The medium was replaced with a fresh one. Then the cells were incubated with $Ru(phen)_3Cl_2$, $Ru(phen)_2(dppz)Cl_2$, MR-**1** and MR-**2** hybrid for 3, 6 and 9 h, respectively. The dishes were then washed with PBS three times. Finally, the cells were observed under a confocal fluorescence microscope.

2.6 *In vitro* toxicity testing for $Ru(phen)_3Cl_2$, $Ru(phen)_2(dppz)Cl_2$, MR-1 and MR-2 hybrid

HeLa cells were cultured in DMEM medium containing 10% FBS, 1% penicillin/streptomycin (complete DMEM) in a humidified atmosphere with 100% humidity and 5% CO_2 at 37 °C. The relative cytotoxicities of $Ru(phen)_3Cl_2$, $Ru(phen)_2(dppz)Cl_2$, MR-**1** and MR-**2** hybrid were evaluated *in vitro* by MTT assay, respectively. HeLa cells were seeded in 96-well plate at a density of 5.0×10^3 cells per well and cultured for 24 h. Subsequently, cells were incubated with $Ru(phen)_3Cl_2$, $Ru(phen)_2(dppz)Cl_2$, MR-**1** and MR-**2** hybrid at different concentrations for 24 h. The cells were washed and the fresh medium containing MTT was added into each plate. The cells were incubated for another 4 h. After that, the medium containing MTT was removed and dimethyl sulfoxide (100 μL) was added to each well to dissolve the formazan crystals. Finally, the plate was gently shaken for 10 min and the absorbance at 490 nm was recorded with a microplate reader.

3 Results and discussion

3.1 Characterization of MSNs, MR-1 and MR-2 hybrid

In order to investigate the interaction between $Ru(phen)_3Cl_2$, $Ru(phen)_2(dppz)Cl_2$ and MSNs, the MSNs, MR-**1** and MR-**2** hybrid was characterized by SEM, TEM, HRTEM mapping, EDS analysis and UV-Vis spectra. SEM, TEM and HRTEM images displayed highly monodisperse and smooth surfaced MSNs, with a mean diameter around 210 nm (Figure 2(a, c) and Figure S1, Supporting Information online). However,

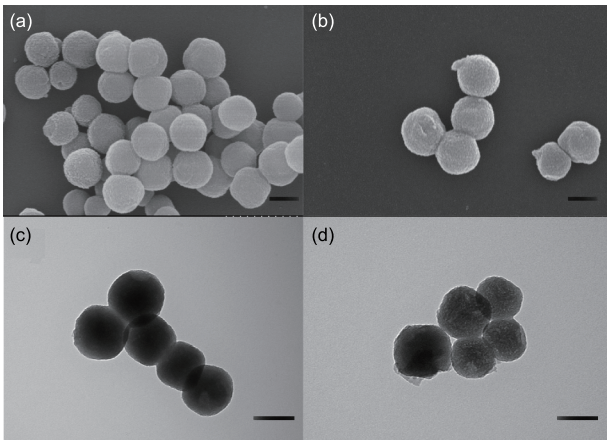

Figure 2 SEM micrographs of (a) MSNs and (b) MR-**1**. Scale bar, 200 nm. TEM micrographs of (c) MSN and (d) MR-**1**. Scale bar, 200 nm.

MR-**1** and MR-**2** hybrid had more rough surfaces (Figure 2(b, d) and Figure S2), suggesting the loading of ruthenium complexes. In order to gain further insight, EDS analysis was also done which revealed the presence of elemental ruthenium besides silicon and oxygen signals, as can be seen in Figure S3. Further, TEM mapping was conducted. As shown in Figure S4, ruthenium complexes were mainly loaded inside the MSNs and a little amount on the surface of MSNs. Moreover, as shown in Figure S5, the peaks at 446 and 440 nm of MR-**1** and MR-**2** were the characteristic peaks of $Ru(phen)_3Cl_2$, $Ru(phen)_2(dppz)Cl_2$ respectively, demonstrating the successful loading of Ru complexes on MSNs.

3.2 Luminescence spectra study

Luminescence spectral properties of $Ru(phen)_3Cl_2$ (1 μM), $Ru(phen)_2(dppz)Cl_2$ (5 μM) alone were examined in 10 mM Tris-HCl buffer (pH 7.4) (Figure S6). $Ru(phen)_3Cl_2$ showed emission maximum at 588 nm whereas $Ru(phen)_2(dppz)Cl_2$ had no emission. To examine the luminescence response of $Ru(phen)_3Cl_2$ and $Ru(phen)_2(dppz)Cl_2$ to DNA, $Ru(phen)_3Cl_2$ and $Ru(phen)_2(dppz)Cl_2$ was titrated with different concentrations of ct-DNA (Figure S6(a, c)) in 10 mM Tris-HCl buffer (pH 7.4). Upon addition of a certain amount of ct-DNA, the emission intensity of $Ru(phen)_3Cl_2$ at 588 nm increased. As for $Ru(phen)_2(dppz)Cl_2$, there gradually appeared a emission peak at 605 nm and enhanced gradually. Moreover, the change of emission intensity of both $Ru(phen)_3Cl_2$ and $Ru(phen)_2(dppz)Cl_2$ had a good linear relationship with the concentration of ct-DNA (Figure S6(b, d)). Then, the MR-**1** containing 1 μM $Ru(phen)_3Cl_2$ and MR-**2** containing 5 μM $Ru(phen)_2(dppz)Cl_2$ were titrated with ct-DNA. As shown in Figure 3, upon addition of a certain amount of ct-DNA into MR-**1** and MR-**2** solution, the emission intensity at 588 nm increased and the emission intensity at 605 nm appeared and

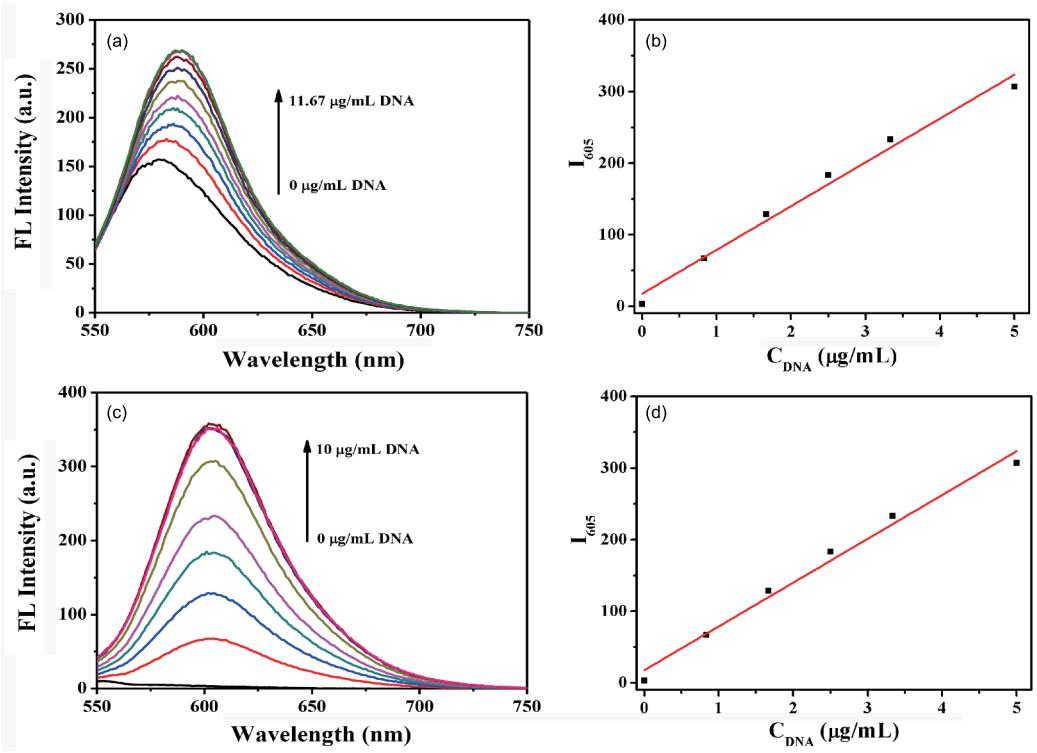

Figure 3 Luminescence titration studies of MR-**1** and MR-**2** upon addition of ct-DNA. (a) Luminescence spectra of MR-**1** (3 mL, 1 μM) upon addition of ct-DNA in Tris-HCl buffer (10 mM, pH 7.4) at room temperature. (b) The linear relationship between the luminescent intensity and ct-DNA concentration. λ_{ex}=465 nm, λ_{em}=588 nm. (c) Luminescence spectra of MR-**2** (3 mL, 5 μM) upon addition of ct-DNA in Tris-HCl buffer (10 mM, pH 7.4) at room temperature. (d) The linear relationship between the luminescent intensity and ct-DNA concentration. λ_{ex}=465 nm, λ_{em}=605 nm (color online).

enhanced accordingly. Both the enhancement also had a good linear relationship with ct-DNA concentration. Specially, there were almost no differences in ct-DNA luminescence titration results between $Ru(phen)_3Cl_2$, $Ru(phen)_2(dppz)Cl_2$ and MR-**1**, MR-**2**, indicating that MSNs have no side effects on the interaction between ruthenium complexes and DNA.

3.3 Cell imaging

The above experimental data indicate that the responses of the MR-**1** and MR-**2** hybrids were almost the same with the responses of $Ru(phen)_3Cl_2$, $Ru(phen)_2(dppz)Cl_2$ alone to DNA. Based on the former reports [48–50], the biocompatible MSNs are better vehicle for the delivery of cancer drugs or bio-macromolecules into live cells by endocytosis. So we further studied the effect of the MR-**1** and MR-**2** in live cells with $Ru(phen)_3Cl_2$, $Ru(phen)_2(dppz)Cl_2$ alone as a control. After 3, 6 and 9 h incubation, luminescence of $Ru(phen)_3Cl_2$, $Ru(phen)_2(dppz)Cl_2$ was detected under 488 nm one-photon excitation using laser confocal microscopes. After 3 h incubation, the luminescence could be observed in the cell nuclei of live cells incubated with the MR-**1** and MR-**2** hybrids and gradually enhanced with the time of incubation (Figure 4). However, there were still no luminescence in live cell nuclei under the control experiments which incubated with $Ru(phen)_3Cl_2$ and $Ru(phen)_2(dppz)Cl_2$ after 9 h incubation (Figure 4). All these can demonstrate that MSNs are good vectors delivering ruthenium complexes into live cells and the MR-**1** and MR-**2** hybrids are good candidates for live cell DNA staining. The efficient delivery of ruthenium complexes into live cells may be attributed to the fact that MSNs can be taken up by cells via energy dependent endocytosis [49].

3.4 Cell toxicity

Further, the MTT assay was conducted in the HeLa cells to confirm the cytotoxicity of $Ru(phen)_3Cl_2$, $Ru(phen)_2(dppz)Cl_2$, MR-**1** and MR-**2**. Figure 5 shows that $Ru(phen)_3Cl_2$, $Ru(phen)_2(dppz)Cl_2$, MR-**1** and MR-**2** all have low toxicity *in vivo* for 24 h. More specific, MR-**1** and MR-**2** have relative lower toxicity than the corresponding $Ru(phen)_3Cl_2$ and $Ru(phen)_2(dppz)Cl_2$ owing to the excellent biocompatibility of MSNs. These all indicated that MSNs

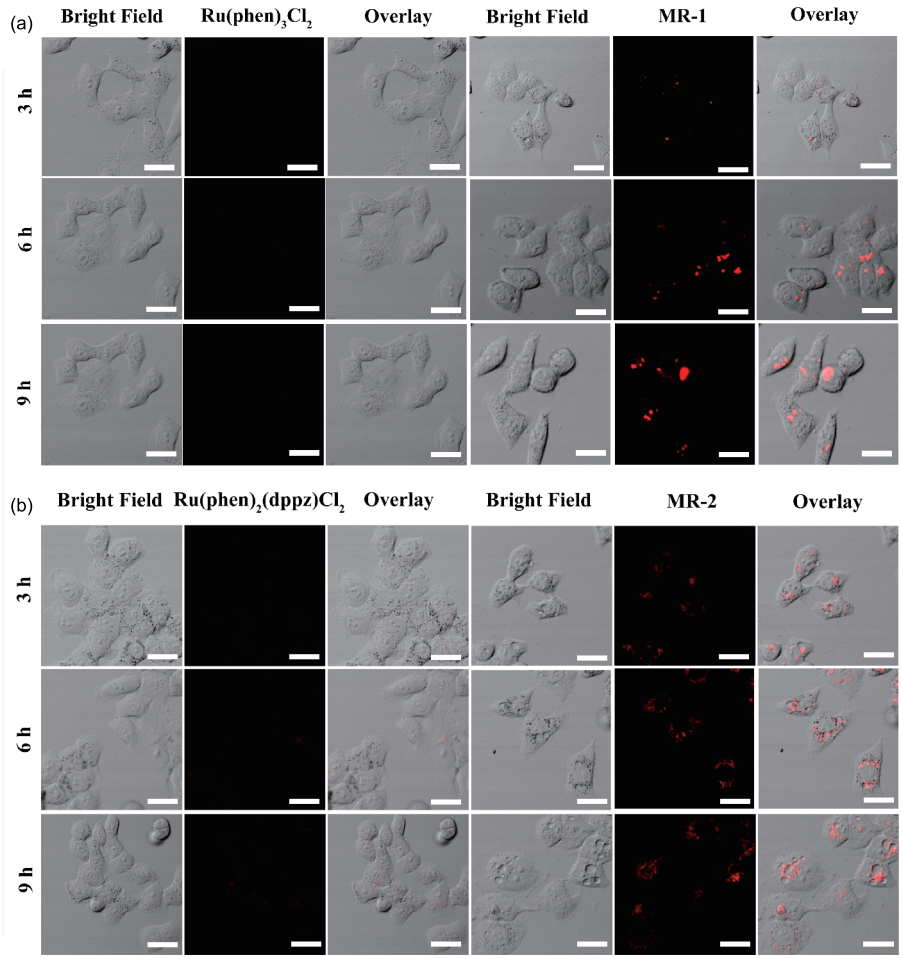

Figure 4 (a) CLSM images of HeLa cells incubated with $Ru(phen)_3Cl_2$ and MR-**1** for 3, 6 and 9 h respectively; (b) CLSM images of HeLa cells incubated with $Ru(phen)_2(dppz)Cl_2$ and MR-**2** for 3, 6 and 9 h respectively. The concentrations of the dyes are all 10 μM. Scale bar: 10 μm (color online).

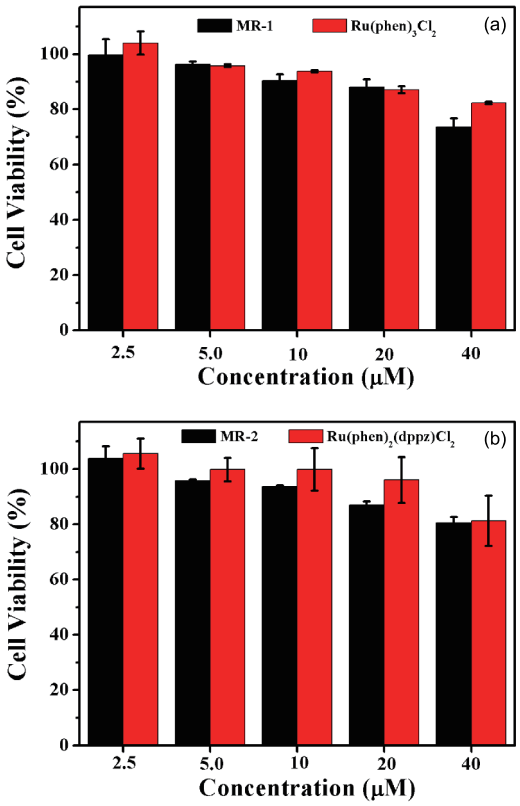

Figure 5 (a) Cytotoxicity of $Ru(phen)_3Cl_2$ and MR-**1** at different concentrations on HeLa cells for 24 h; (b) cytotoxicity of $Ru(phen)_2(dppz)Cl_2$ and MR-**2** at different concentrations on HeLa cells for 24 h (color online).

not only acted as vectors but also contributed to reducing the toxicity of ruthenium complexes.

4 Conclusions

In summary, MSNs and the corresponding ruthenium complexes can be bonded non-covalently to form physical adsorption MSNs-Ru materials, which had no side effects on the interactions between Ru complexes and DNA. MSNs were exploited as an efficient nano-vehicle for loading and delivery of these ruthenium complexes into live cells to stain DNA while ruthenium complexes alone can hardly enter into live cells. Collectively, this work provides further insight into the design of efficient MSNs-based delivery systems for biological applications.

Acknowledgments This work was supported by the Scientific Research Foundation of Northwest A&F University (Z111021103, Z111021107), and the National Natural Science Foundation of China (21472016, 21272030, 21476185).

Conflict of interest The authors declare that they have no conflict of interest.

Supporting information The supporting information is available online at http://chem.scichina.com and http://link.springer.com/journal/11426. The supporting materials are published as submitted, without typesetting or editing. The responsibility for scientific accuracy and content remains entirely with the authors.

1 Svozil D, Kalina J, Omelka M, Schneider B. *Nucleic Acids Res*, 2008, 36: 3690–3706
2 Lo KKW, Choi AWT, Law WHT. *Dalton Trans*, 2012, 41: 6021–6047
3 Shamsipur M, Memari Z, Ganjali MR, Norouzi P, Faridbod F. *J Pharmaceut Biomed Anal*, 2016, 118: 356–362
4 Wang L, Liu S, Hao C, Zhang X, Wang C, He Y. *Sensor Actuat B-Chem*, 2016, 229: 145–154
5 Chu C, Wang X, Li S, Ge S, Ge L, Yu J, Yan M. *Anal Methods*, 2012, 4: 4339–4345
6 Wang Q, Xu N, Lei J, Ju H. *Chem Commun*, 2014, 50: 6714–6717
7 Lo K, Tsang K, Sze K, Chung C, Lee T, Zhang K, Hui W, Li C, Lau J, Ng D. *Coordin Chem Rev*, 2007, 251: 2292–2310
8 Lo KKW, Zhang KY, Leung SK, Tang MC. *Angew Chem Int Ed*, 2008, 47: 2213–2216
9 Capodilupo AL, Vergaro V, Accorsi G, Fabiano E, Baldassarre F, Corrente GA, Gigli G, Ciccarella G. *Tetrahedron*, 2016, 72: 2920–2928
10 Norton AB, Hancocks RD, Spyropoulos F, Grover LM. *Food Hydrocolloid*, 2016, 53: 93–97
11 Liao G, Chen X, Wu J, Qian C, Wang Y, Ji L, Chao H. *Dalton Trans*, 2015, 44: 15145–15156
12 Rajendiran V, Palaniandavar M, Periasamy VS, Akbarsha MA. *J Inorg Biochem*, 2010, 104: 217–220
13 Hu P, Wang Y, Zhang Y, Song H, Gao F, Lin H, Wang Z, Wei L, Yang F. *RSC Adv*, 2016, 6: 29963–29976
14 Zhang Y, Hu PC, Cai P, Yang F, Cheng GZ. *RSC Adv*, 2015, 5: 11591–11598
15 Nithyakumar A, Alexander V. *New J Chem*, 2016, 40: 4606–4616
16 Lo KKW, Li SPY. *RSC Adv*, 2014, 4: 10560–10585
17 Li G, Sun L, Ji L, Chao H. *Dalton Trans*, 2016, 45: 13261–13276
18 Li H, Wen J, Yu R, Meng J, Wang C, Wang C, Sun S. *RSC Adv*, 2015, 5: 9341–9347
19 Li H, Wen J, Yu R, Bai C, Xu Y, Liu ZH, Sun S. *RSC Adv*, 2015, 5: 26856–26862
20 Gill MR, Thomas JA. *Chem Soc Rev*, 2012, 41: 3179–3192
21 Balakrishnan G, Rajendran T, Senthil Murugan K, Sathish Kumar M, Sivasubramanian VK, Ganesan M, Mahesh A, Thirunalasundari T, Rajagopal S. *Inorg Chim Acta*, 2015, 434: 51–59
22 Liu P, Wang X, Hiltunen K, Chen Z. *ACS Appl Mater Interfaces*, 2015, 7: 26811–26818
23 Chen WX, Song XD, Chen JX, Zhao XH, Xing JH, Ren JR, Wu T, Sun J. *Polyhedron*, 2016, 110: 274–281
24 Zhao XL, Li ZS, Zheng ZB, Zhang AG, Wang KZ. *Dalton Trans*, 2013, 42: 5764–5777
25 Tan L, Shen J, Liu J, Zeng L, Jin L, Weng C. *Dalton Trans*, 2012, 41: 4575–4587
26 Thota S, Vallala S, Yerra R, Rodrigues DA, Raghavendra NM, Barreiro EJ. *Int J Biol Macromol*, 2016, 82: 663–670
27 El-Sonbati AZ, Shoair AF, El-Bindary AA, Diab MA, Mohamed AS. *J Mol Liq*, 2015, 209: 635–647
28 Kumar A, Kumar A, Gupta RK, Paitandi RP, Singh KB, Trigun SK, Hundal MS, Pandey DS. *J Organomet Chem*, 2016, 801: 68–79
29 Li HJ, Liu FY, Sun SG, Wang JY, Li ZY, Mu DZ, Qiao B, Peng XJ. *J Mater Chem B*, 2013, 1: 4146–4151
30 Liu F, Gao Y, Li H, Sun S. *Carbon*, 2014, 71: 190–195
31 Li Z, Sun S, Yang Z, Zhang S, Zhang H, Hu M, Cao J, Wang J, Liu F,

Song F, Fan J, Peng X. *Biomaterials*, 2013, 34: 6473–6481
32 Popat A, Ross BP, Liu J, Jambhrunkar S, Kleitz F, Qiao SZ. *Angew Chem Int Ed*, 2012, 51: 12486–12489
33 Slowing II, Trewyn BG, Lin VSY. *J Am Chem Soc*, 2007, 129: 8845–8849
34 Han N, Wang Y, Bai J, Liu J, Wang Y, Gao Y, Jiang T, Kang W, Wang S. *Microporous Mesoporous Mater*, 2016, 219: 209–218
35 Yuan Q, Zhang Y, Chen T, Lu D, Zhao Z, Zhang X, Li Z, Yan CH, Tan W. *ACS Nano*, 2012, 6: 6337–6344
36 Sinha A, Jana NR. *Eur J Inorg Chem*, 2012, 2012: 4470–4478
37 Walcarius A. *Electroanalysis*, 2015, 27: 1303–1340
38 Deng Y, Wei J, Sun Z, Zhao D. *Chem Soc Rev*, 2013, 42: 4054–4070
39 Chen HW, Chiang YD, Kung CW, Sakai N, Ikegami M, Yamauchi Y, Wu KCW, Miyasaka T, Ho KC. *J Power Sources*, 2014, 245: 411–417
40 Zhou Z, Hartmann M. *Chem Soc Rev*, 2013, 42: 3894–3912
41 Wu SH, Mou CY, Lin HP. *Chem Soc Rev*, 2013, 42: 3862–3875
42 Colilla M, González B, Vallet-Regí M. *Biomater Sci*, 2013, 1: 114–134
43 Chen H, Zheng D, Liu J, Kuang Y, Li Q, Zhang M, Ye H, Qin H, Xu Y, Li C, Jiang B. *Int J Biol Macromol*, 2016, 85: 596–603
44 Niemelä E, Desai D, Nkizinkiko Y, Eriksson JE, Rosenholm JM. *Eur J Pharm Biopharm*, 2015, 96: 11–21
45 Teng Z, Han Y, Li J, Yan F, Yang W. *Microporous Mesoporous Mater*, 2010, 127: 67–72
46 Westerlund F, Pierard F, Eng MP, Nordén B, Lincoln P. *J Phys Chem B*, 2005, 109: 17327–17332
47 Dickeson J, Summers L. *Aust J Chem*, 1970, 23: 1023–1027
48 Zhang X, Zhang X, Wang S, Liu M, Zhang Y, Tao L, Wei Y. *ACS Appl Mater Interfaces*, 2013, 5: 1943–1947
49 Wang Y, Zhao Q, Han N, Bai L, Li J, Liu J, Che E, Hu L, Zhang Q, Jiang T, Wang S. *Nanomed-Nanotechnol Biol Med*, 2015, 11: 313–327
50 Zhu CL, Lu CH, Song XY, Yang HH, Wang XR. *J Am Chem Soc*, 2011, 133: 1278–1281